for dissolved aluminium with respect to scavenging calculated from the deep North Pacific profiles is similar. With respect to the best estimate of riverine input[24] the residence time is only 40 yr. However, this approach is not entirely valid due to the fact that dissolved aluminium delivered by rivers may be largely removed in the estuaries[25-27] and coastal zone, and fluvial input may not be a large net source of dissolved aluminium to the central oceans.

We conclude that the concentration of dissolved aluminium is 8-40 times lower in the central North Pacific than in the central North Atlantic. No other element has been reported to show an enrichment in the Atlantic over the Pacific of this great a magnitude. This interbasin difference seems to be due to the short residence time of dissolved aluminium coupled with the differences in atmospheric input, though more work is needed to understand fully the processes involved. Estimates of the mean oceanic concentration of dissolved aluminium must be lowered from 20-70 to ~2 nmol kg^{-1}. Estimated residence times are all short (<200 yr) supporting the conclusion that dissolved aluminium, probably in the form of $Al(OH)_3^0$ and $Al(OH)_4^-$, is an extremely particle-reactive element in the ocean. Although there is *in situ* scavenging throughout the water column, regeneration of dissolved aluminium at or near the sediment interface results in increased concentrations in the bottom waters.

We thank Rob Franks and Margaret Delaney for their critical review of this paper, and Geoff Smith for help with sample collection. This research was supported by NSF grant OCE-8216672.

Received 29 January; accepted 5 June 1985.

1. Taylor, S. R. *Geochim. cosmochim. Acta* **28**, 1273-1285 (1964).
2. Bruland, K. W. in *Chemical Oceanography*, Vol. 8 (eds Riley, J. P. & Chester, R.) 157-220 (Academic, London, 1983).
3. Hydes, D. J. *Science* **205**, 1260-1262 (1979).
4. Hydes, D. J. *Geochim. cosmochim. Acta* **47**, 967-973 (1983).
5. Moore, R. M. *Geochim. cosmochim. Acta* **45**, 2475-2482 (1981).
6. Olafsson, J. in *Trace Metals in Seawater* (eds Wong, C. S., Boyle, E., Bruland, K. W., Burton, J. D. & Goldberg, E. D.) 475-485 (Plenum, New York, 1983).
7. Measures, C. I., Grant, B., Khadem, M., Lee, D. S. & Edmond, J. M. *Earth planet. Sci. Lett.* **71**, 1-12 (1984).
8. Stoffyn, M. *Science* **203**, 651-653 (1979).
9. Hydes, D. J. *Nature* **268**, 136-137 (1977).
10. Goldberg, E. D., Broecker, W. S., Gross, M. G. & Turekian, K. K. in *Radioactivity in the Marine Environment*, 137-146 (National Academy of Sciences, Washington DC, 1971).
11. Neihof, R. A. & Loeb, G. I. *J. mar. Res.* **32**, 5-12 (1974).
12. MacKenzie, F. T., Stoffyn, M. & Wollast, R. *Science* **199**, 680-682 (1978).
13. Stoffyn, M. *Science* **203**, 651-653 (1979).
14. Stoffyn, M. & Mackenzie, F. T. *Mar. Chem.* **11**, 105-127 (1982).
15. Schutz, L., Jaenicke, R. & Pietrek, H. *Geol. Soc. Am. Spec. Pap.* **186**, 87-100 (1981).
16. Chester, R. *Mar. Chem.* **11**, 1-16 (1982).
17. Hodge, V., Johnson, S. R. & Goldberg, E. D. *Geochem. J.* **12**, 7-20 (1978).
18. Craig, H. *Earth planet. Sci. Lett.* **23**, 149-159 (1974).
19. Broecker, W. S. & Peng, T. *Tracers in the Sea*, 236-243 (Eldigio, New York, 1982).
20. Lewin, J. C. *Geochim. cosmochim. Acta* **21**, 182-198 (1961).
21. Stoffyn-Elgi, P. *Geochim. cosmochim. Acta* **46**, 1345-1352 (1982).
22. Whitfield, M. *Interdis. Sci. Rev.* **6**, 12-35 (1981).
23. Quinby-Hunt, M. S. & Turekian, K. K. *EOS* **64**, 130-131 (1983).
24. Martin, J. M. & Whitfield, M. in *Trace Metals in Seawater*, (eds Wong, C. S., Boyle, E., Bruland, K. W., Burton, J. D. & Goldberg, E. D.) 265-296 (Plenum, New York, 1983).
25. Hydes, D. J. & Liss, P. S. *Estuar. coast. mar. Sci.* **5**, 755-769 (1977).
26. Scholkovitz, E. R. *Earth planet. Sci. Lett.* **41**, 77-86 (1978).
27. Mackin, J. E. & Aller, R. C. *Mar. Chem.* **14**, 213-232 (1984).
28. Prospero, J. M. in *The Sea*, Vol. 7 (ed. Emiliani, C.) 801-874 (Wiley, New York, 1981).
29. Buat-Menard, P. & Chesselet, R. *Earth planet. Sci. Lett.* **42**, 399-411 (1979).
30. Uematsu, M. *et al. J. geophys. Res.* **88**, 5343-5352 (1983).
31. Bruland, K. W., Franks, R. P., Knauer, G. A. & Martin, J. H. *Analyt. chim. Acta* **105**, 233-245 (1979).
32. Bruland, K. W. *Earth planet. Sci. Lett.* **47**, 176-198 (1980).

Age and palaeoclimatic significance of the loess of Lanzhou, north China

Douglas W. Burbank

Department of Geological Sciences, University of Southern California, Los Angeles, California 90089-0741, USA

Li Jijun

Department of Geology and Geography, Lanzhou University, Lanzhou, Gansu, People's Republic of China

Extending in a broad arc that abuts the sandy (non-Gobi) deserts, the loess plateau of northern China[1-3] is one of the most massive accumulations of loess in the world. The loess sequence is typically characterized by an alternation of silty or sandy loess with more clay-rich palaeosols. These alternations, in conjunction with their enclosed faunas and distinctive mineralogies, have been interpreted as reflecting Pleistocene glacial/interglacial cycles[3-8]. Because it holds implications for the climatic and anthropological history of China[9,10], the definition of a reliable chronological framework for loess deposition is of great interest. Recent palaeomagnetic studies[4,5] have indicated that loess deposition in Shaanxi province commenced ~2.4 Myr ago. To assess the synchrony of loess accumulation across the loess plateau, we have dated a 330-m-thick loess sequence near Lanzhou, Gansu province. The magnetostratigraphical results reported here indicate that the base of this loess succession dates from ~1.3 Myr ago. This young age (in comparison to the Shaanxi sequence) is attributed to uplift along the northern fringe of the Tibetan Plateau[11] that precluded early Pleistocene loess preservation in this mountainous region. Palaeosols in the basal loess occur, on average, once every 25 kyr, suggesting that climates conducive to soil-forming events may have been modulated by orbital precession in the early Pleistocene.

Within the extensive loess plateau (Fig. 1*a*), the best-documented loess successions are in Shaanxi province[1,9], where the loess mantle averages 80-140 m in thickness (Fig. 1*b*). Recent magnetostratigraphical investigations at Luochuan in Shaanxi[4,5] have indicated that loess deposition commenced ~2.4 Myr ago, a date remarkably similar to the timing of both the initiation of loess deposition in Europe[12,13] and the isotopically-determined onset of major Northern Hemisphere glaciation[14]. Given this apparently synchronous response on a global scale to Plio-Pleistocene climatic change, it might be assumed that the loess of north China spans a consistent chronological interval throughout most of its areal extent.

To test this assumption, we have created a magnetostratigraphy for the loess sequence at Lanzhou, 500 km to the west of Luochuan (Fig. 1*b*). At Lanzhou, the highest fluvial terrace of the Huang Ho is overlain by >330 m of loess and appears to be the oldest loess-mantled surface in the area. Wang's[15] palaeomagnetic studies of this sequence used alternating-field (a.f.) demagnetization, placed the Brunhes/Matuyama boundary 105 m above the base, delineated three normal magnetozones in the late Matuyama chron, and indicated increasingly dispersed magnetic orientations (suggestive of incomplete overprint removal) in strata older than 500 kyr. In the present study, the lowermost 100 m of loess were sampled along the completely exposed walls of a steep gully. In the succeeding 230 m, pits up to 5 m deep were excavated to obtain samples of the undisturbed loess from beneath any colluvial material. Palaeomagnetic sampling sites, comprising three or four specimens each, were spaced at ~7-m intervals and, wherever possible, were chosen so as to avoid palaeosols. Pilot studies using stepwise a.f. and thermal demagnetization indicate that: (1) some reversely magnetized specimens exhibit a soft, viscous overprinting of normal polarity; (2) this overprinting can usually be removed at low demagnetization levels (150 Oe or 200 °C); (3) above these levels, most specimens exhibit a stable characteristic remanence; and (4) the primary magnetic carrier appears to be magnetite or titanomagnetite with minor contributions from haematite.

Because a.f. demagnetization successfully revealed the characteristic remanence in most cases, all specimens were demagnetized at 200 Oe. Subsequently, the reliability of the mean magnetic orientation at each site was statistically evaluated[16] and classified[17] as either 'Class I' (Fisher $k \geq 10$), 'Class II' ($k < 10$, but two samples in close agreement), or 'Class III' (unreliable). All specimens from 'Class II' sites and all normally polarized specimens below the Brunhes/Matuyama boundary were subjected to stepwise thermal demagnetization. This resulted in

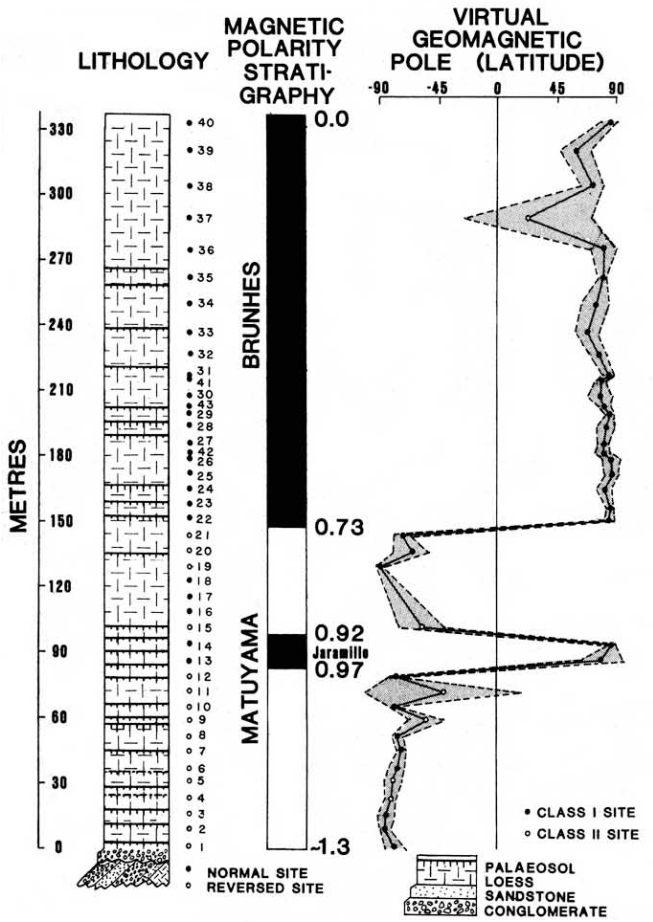

Fig. 1 *a*, Location map indicating the distribution of loess in north China, the loess plateau, and the mountain ranges. The loess plateau, covering >300,000 km^2, is rimmed on three margins by mountain ranges and to the north is open to the sandy deserts of the southern Gobi Desert. *b*, The age, distribution, and thickness of loess in the central and western loess plateau. The mean grain size of the loess diminishes to the south away from the source of the loess, the sandy Tengger and Mu Us deserts along the southern margin of the greater Gobi Desert. The magnetic polarity stratigraphy and thickness of the loess profiles at Lanzhou in Gansu province and Luochuan in Shaanxi province are depicted by the vertical columns. The time-correlation lines drawn between them illustrate the rapid attenuation of loess-accumulation rates (from 26 to 7 cm kyr^{-1}) attributed to increasing distance from the source of the loess.

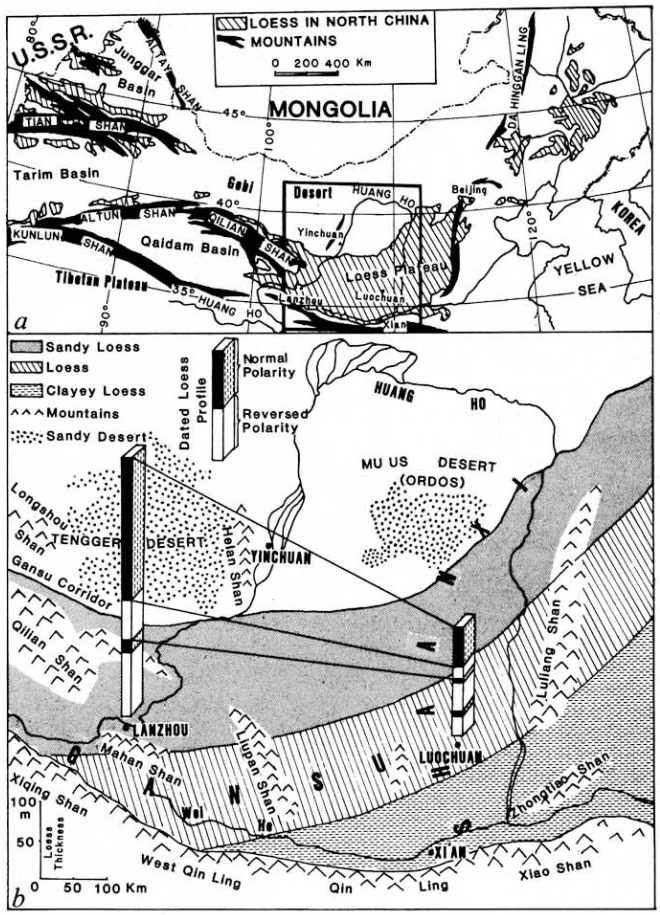

Fig. 2 Lithologies and the magnetic polarity stratigraphy (MPS) from the Lanzhou loess sequence. Only the lower 100 m of the succession are completely exposed. The number of palaeosols depicted in the upper 230 m reflects those occurring near sampling sites and probably underestimates their true abundance. Sampling site numbers (referred to in the text) are shown adjacent to the lithological column. The latitude (degrees) of the virtual geomagnetic pole (VGP) is based on the mean inclination and declination of each site. An α_{95} confidence envelope is plotted (shading) around each VGP latitude. As discussed in the text, sites 16–18 are not included in the VGP or MPS plots. The ages (Myr) of the magnetic boundaries are based on refs 17 and 18. The age of the basal loess is estimated by extrapolation of the mean loess-accumulation rate.

more concordant directions for the specimens from several sites and confirmed the normal polarity of five sites in the basal portion of the sequence.

The resulting magnetostratigraphy for the Lanzhou loess is shown in Fig. 2. It comprises 34 Class I sites and 6 Class II sites. Three Class I sites (16–18, Fig. 2) are not included in the magnetic zonation and are discussed below. The latitude of the virtual geomagnetic pole (VGP) is used to define the polarity of each site. The α_{95} confidence envelope plotted for each VGP latitude (Fig. 2) indicates a high level of reliability for most sites. The uppermost normal magnetozone is interpreted as the Brunhes chron, which overlies reversed magnetozones attributed to the Matuyama chron. The Jaramillo normal subchron is defined by sites 13 and 14. Calculations of mean loess-accumulation rates between reversal boundaries of known ages[18,19] consistently yield a value averaging 26 cm kyr^{-1} for the past million years. Extrapolation of this rate to the base of the Lanzhou loess sequence suggests that it dates from ~1.3 Myr ago. These results differ from the earlier magnetostratigraphical studies of Wang[15] in that the Brunhes/Matuyama boundary is placed 50 m higher, the base of the sequence is estimated to be 200–300 kyr older, and the reliability of the sites (as defined by the α_{95}-error envelope, Fig. 2) remains high throughout the sequence. The absence of Wang's lower two normal magnetozones (between 40 and 75 m, Fig. 2) within the reversely magnetized sediments below the Jaramillo subchron may be attributable to thermal demagnetization that revealed a characteristic reversed remanence for many specimens that had displayed dispersed normal polarities following a.f. demagnetization.

In an effort to provide data on an inaccessible portion of our main section (105–125 m, Fig. 2), three sites were collected from scarps ringing collapse pits 100 m west of the primary sampling gully. These normally magnetized sites (16–18, Fig. 2) were not included in the magnetostratigraphy for the following reasons: (1) their stratigraphical position is uncertain due to covered strata obscuring possible unconformities[12,13]; (2) they may have slumped from Brunhes-aged strata above; and (3) their inclusion would render the magnetostratigraphy less interpretable. Furthermore, our laboratory experiments indicate that periodic wetting to near saturation can cause the magnetic orientation of loess specimens to shift dramatically over periods of less than a week towards the ambient field direction. The amount and stability of the shift appears to be an inverse function of the degree of lithification. The older, well lithified specimens appear

largely unaffected by wetting. In contrast, the major magnetic contributors to the remanence of the younger specimens, including some from sites 16-18, rotate partially or completely into the ambient field direction and are directionally stable against at least a 1,000-Oe demagnetizing field. In natural situations, these experimental results imply that gradual lithification and removal from the zone of periodic wetting by burial are both important components in 'locking in' the characteristic remanence. Because the partially indurated specimens from sites 16-18 lie along collapse pits that were formed by and presently act as conduits for runoff, there is a strong possibility that their characteristic remanence has been reoriented. Consequently, these sites are excluded from the magnetostratigraphy. The specimens from the overlying sites were collected at least 2 m below the modern surface, where they were below the zone of natural wetting and, hence, are unlikely to have been reoriented.

A comparison of the results from Lanzhou with those from Luochuan (Fig. 1*b*) yields some new insights into the nature of loess deposition in China. Large, modern dustfalls tend to originate in the northern deserts and to distribute loess across the entire loess plateau[20]. Similarly, ancient loess deposition beginning in the late Pliocene[4,5] is likely to have been generally synchronous across the loess plateau. Our study indicates, however, that the oldest preserved loess can vary in age between regions by as much as 1 Myr. We attribute these differences to Plio-Pleistocene uplift of the Tibetan Plateau[11,21] which caused structural disruption of its marginal regions, including those around Lanzhou. Although the ongoing Indo/Asian collision continues to deform north China[22,23], major deformation appears to have been transferred out of the Lanzhou basin after the early Pleistocene.

Whereas the loess-accumulation rates have averaged 7 cm kyr^{-1} at Luochuan since the Jaramillo subchron, the mean rate at Lanzhou has been nearly four times higher during the same interval. This high rate and the remarkable thickness of the Lanzhou loess is explained both by its proximity to the northern deserts and by the local topography, whereby dust-laden, high-velocity winds funnelled through the Gansu Corridor (Fig. 1*b*) and over Wushaoling Pass expand, decelerate, and release some of their sediment load in the Lanzhou basin. The coarser mean grain size of the Lanzhou loess, when compared to the silty (Luochuan) or clay-rich (Xian) loess farther south (Fig. 1*b*), reflects similar causes. Palaeomagnetic studies at Luochuan[4,5] indicate that haematite is the primary magnetic carrier and that it results from *in situ* chemical processes related to lesser or greater amounts of soil formation. In Lanzhou, the high rates of loess accumulation generally overwhelmed the soil-forming process. Consequently, detrital magnetite or titanomagnetite, rather than chemical haematite, is the primary magnetic mineral. Finally, within the completely exposed, lower 100 m of the Lanzhou sequence, 15 weakly to moderately developed palaeosols are preserved (Fig. 2). Given the calculated accumulation rates, one soil-forming episode would have occurred approximately every 25 kyr. This frequency is very similar to that determined for the precession of the equinoxes[24] and may, thus, reflect control exerted by Milankovitch-type orbital parameters[25] on the early Pleistocene climates of north China.

This study was supported by the Lanzhou University and the Shell Foundation provided support to Douglas W. Burbank. During the experimental studies, Li Jijun was supported as a visiting scholar to the University of Southern California by Lanzhou University. Helpful discussions with S. Lund and a review by F. Theyer are gratefully acknowledged.

Received 19 March; accepted 10 June 1985.

1. Liu, T. S. & Chang, T. H. *Rep. 6th int. Congr. Quat. Warsaw* **6**, 503-524.
2. Liu, T. S., Wang, T. M., Wang, K. L. & Wen, L. C. *Sci. Rec.* **2**, 167-174 (1958).
3. Sasajima, S. & Wang, Y. Y. *The Recent Research of Loess in China* (Kyoto University and Northwest University, 1984).
4. Heller, F. & Liu, T. S. *Nature* **300**, 431-433 (1982).
5. Heller, F. & Liu, T. S. *Geophys. J. R. astr. Soc.* **77**, 125-141 (1984).
6. Chen, D. N. *et al. Proc. 3rd Nat. Quat. Congr.*, China (1979).
7. Liu, T. S., Wen, O. Z., An, Z. S. & Zheng, H. H. *Int. geol. Congr.*, Paris (1980).
8. Zheng, H. H., in *Quaternary Geology and Environment of China* (ed. Liu, T. S.) 59-66 (China Ocean Press, Beijing, 1982).
9. Woo, R. K. *Kexue Tongbao* **6**, (1966).
10. Wang, Y. Y. & Xue, S. S. in *Loess and Quaternary Geology* (ed. Wang, Y. Y.) 88-98 (People's Press, Shaanxi Province, Xian, 1982).
11. Li, J. *et al. Scient. Sinica* **22**, 1314-1328 (1979).
12. Kukla, G. J. in *After the Australopithecines* (eds Butzer, K. W. & Issac, G. L.) 99-188 (Mouton, The Hague, 1975).
13. Fink, J. & Kukla, G. *J. Quat. Res.* **7**, 363-371 (1977).
14. Shackleton, N. J. *et al. Nature* **307**, 620-623 (1984).
15. Wang, Y. Y., in *Loess and Quaternary Geology* (ed. Wang, Y. Y.) 20-47 (People's Press, Shaanxi, 1982).
16. Fisher, R. A. *Proc. R. Soc.* **A217**, 295-305 (1953).
17. Johnson, N. M. *et al. Palaeogeogr., Palaeoclimatol., Palaeoecol.* **37**, 17-42 (1982).
18. Mankinen, E. A. & Dalrymple, G. B. *J. geophys. Res.* **84**, 615-626 (1979).
19. Harland, W. B. *et al. A Geologic Time Scale* (Cambridge University Press, 1982).
20. Liu, T. S., Gu, X. F., An, Z. S. & Fang, Y. X. in *Desert Dust: origin Characteristics and Effect on Man* (ed. Pewe, T. L.) 149-158 (Geological Society of America, Boulder, 1981).
21. Xu, R. in *Geological and Ecological Studies of the Qinghai-Xizang Plateau* Vol. 1 139-144 (Science Press, Beijing, 1981).
22. Tapponier, P. & Molnar, P. *J. geophys. Res.* **82**, 2905-2930 (1977).
23. Molnar, P. & Tapponier, P. *J. geophys. Res.* **83**, 5361-5375 (1978).
24. Berger, A. in *Milankovitch and Climate, Part I* (eds Berger, A., Imbrie, J., Hays, J., Kukla, G. & Saltzman, B.) 3-39 (Reidel, Dordrecht, 1984).
25. Hays, J. D., Imbrie, J. & Shackleton, N. J. *Science* **214**, 1121-1132 (1976).

Effect of drought on dust production in the Sahel

N. J. Middleton

School of Geography, University of Oxford, Mansfield Road, Oxford OX1 3TB, UK

The severe drought currently afflicting the Sudano–Sahelian zone to the south of the Sahara Desert has been suggested to be instrumental in producing an increased output of soil-derived aerosols into the atmosphere from the region[1]. During the very dry period 1972–74 mean aerosol concentrations at Barbados, West Indies, as affected by the African Dust Plume[2], were three times that of pre-drought levels[1], that is before 1968. A marked increase in the frequency of severe dust occurrences in northern Nigeria has also been noted during 1972 and 1973 (ref. 3). I present here data from selected meteorological stations which show that dust-storm activity in the west and east of the Sudano–Sahelian belt has dramatically increased during the drought years; by a factor of 6 in Mauritania and up to a factor of 5 in Sudan.

The Sudano-Sahelian zone lies approximately between latitudes 10 and 20° N and includes parts of Mauritania, Senegal, Mali, Burkina Faso, Niger, Chad, Sudan and Ethiopia. Study of the zone is impaired by a general lack of adequate long-term data for large parts of its area, but data for Mauritania in the west and Sudan in the east have made this investigation possible.

Perhaps the most striking representation of an increase in dust-raising activity with the onset of drought conditions is shown in Fig. 1. This shows the variation of annual dust-storm frequency and annual rainfall totals for Nouakchott in Mauritania and El Fasher in Sudan. At Nouakchott, and generally for Mauritanian stations south of ~20° N, dust-storm activity is largely concentrated in the period from January to May, before the onset of the rainy season. At this time of year, dust concentrations at Barbados are relatively low[1], but the dust concentration measured at Cayene, French Guiana[4] is at a maximum. (North of 20° N, where the rainy season starts later in the year, maximum dust-storm activity starts in February and continues until July or August.) Low rainfall totals of 48.1 mm in 1970 and 17.9 mm in 1971 represented just 32 and 12%, respectively, of the 1949-67 average, and can be seen as the main onset of the drought. The number of dust-storm days increased dramatically from 6 in 1970 to 65 in 1974 before a reasonably high annual rainfall of 190.6 mm in 1975; dust-storm activity declined to 25 days in 1976 and 27 days in 1977. In 1977, the rainy season brought only 2.7 mm of precipitation, however, making it the driest year since records began in 1931, and dust-storm activity rose to 55 and 61 days in 1978 and 1979 respectively. The total dropped to 33 dust-storm days in 1980 after a relatively heavy rainfall in 1979, but rose to an unprecedented 85 days in 1983 as rainfall again diminished.

A similar pattern is shown in the graph for El Fasher in the eastern Sahel (Fig. 1*b*). Here particularly low rainfall in 1972 and 1973 was followed by a distinct rise in dust-storm frequency